JACS
JOURNAL OF THE AMERICAN CHEMICAL SOCIETY

Communication

pubs.acs.org/JACS

Harnessing Molecular Photon Upconversion in a Solar Cell at Sub-solar Irradiance: Role of the Redox Mediator

Sean P. Hill and Kenneth Hanson*

Department of Chemistry and Biochemistry, Florida State University, Tallahassee, Florida 32306, United States

Supporting Information

ABSTRACT: Self-assembled bilayers offer a promising strategy to directly harness photon upconversion via triplet−triplet annihilation (TTA-UC) and increase maximum theoretical solar cell efficiencies from 33% to >43%. Here we demonstrate that the choice of redox mediator in these solar cells has a profound influence on both the light harvesting and TTA-UC efficiency. Devices with $Co^{II/III}(phen)_3$ as the redox mediator produced the highest photocurrent yet generated from TTA-UC (0.158 mA cm^{-2}) under 1 sun. Despite generating less photocurrent, $Co^{II/III}(pz\text{-}py\text{-}pz)_2$ devices achieved maximum TTA-UC efficiency at excitation intensities well below solar irradiance (0.8 mW cm^{-2}), which is on par with the lowest value yet reported for any TTA-UC system. The large variation in performance with respect to mediator is attributed to triplet excited-state quenching via (1) energy transfer or paramagnetic quenching by the Co^{II} species and (2) excited-state electron transfer to Co^{III} species.

Due to fundamental physical limitations, the maximum theoretical efficiency of a single junction solar cell is approximately 33% as originally outlined by Shockley and Queisser.[1] This limit is derived by maximizing the power output of the cell (photovoltage multiplied by photocurrent) under solar irradiance. High voltages can be achieved by using large band gap materials but transmission of low-energy, sub-band-gap light limits photocurrent generation. Harnessing this low-energy light via photon upconversion (UC) can compensate for these transmission/photocurrent losses and can increase the maximum theoretical efficiencies to >43%.[2] Molecular photon UC by way of triplet−triplet annihilation (TTA-UC)[3] is of particular interest because it can be an efficient process even under low-intensity, noncoherent solar irradiance.[4]

Current efforts to harness TTA-UC for solar energy conversion can be partitioned into either optical or electronic coupling schemes. In the former, photocurrent enhancements of up to 0.0045 mA cm^{-2},[5] under 1 sun, have been demonstrated by exploiting a TTA-UC filter/reflector that absorbs the transmitted light and directs the UC emission back to the solar cell.[4b,6] In contrast, the electronically coupled arrangement involves directly extracting charge from the upconverted state, prior to emission, effectively integrating TTA-UC into solar cell architectures such as dye-sensitized solar cells (DSSCs)[7] or organic photovoltaics.[8] Regardless of the device scheme, for real world applications it is crucial that these devices achieve photocurrent enhancements >0.1 mA cm^{-2} at solar or sub-solar intensities.[9]

Recently, our group introduced self-assembled molecular multilayers[10] on metal oxide surfaces[11] as an effective means of facilitating TTA-UC emission and charge separation.[12] The bilayer films, assembled through stepwise soaking, are composed of 4,4′-(anthracene-9,10-diyl)bis(4,1-phenylene)-diphosphonic acid as the acceptor molecule (A), and Pt(II)-tetrakis(4-carboxyphenyl)porphyrin as the sensitizer (S) coordinated via ion linkage as depicted in Figure 1. With

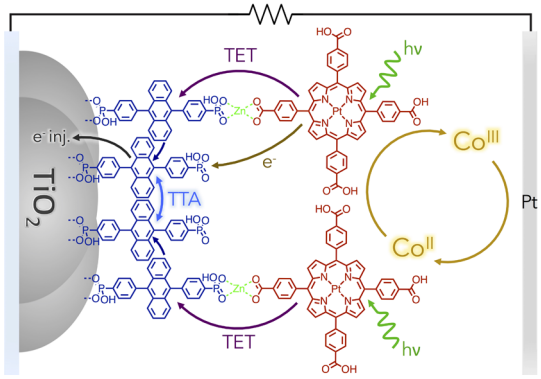

Figure 1. Schematic representation of the self-assembled bilayer (TiO_2−A−Zn−S) in a DSSC with cobalt-based redox mediator. (TET = triplet energy transfer and TTA = triplet−triplet annihilation.)

these bilayers[7b] or dual sensitized trilayers[13] as the anode of TTA-UC DSSCs, we have demonstrated photocurrent enhancements of 0.009 and 0.074 mA cm^{-2}, respectively, under 1 sun irradiation (AM1.5). While still relatively low, these values are approaching the device relevant photocurrent threshold of 0.1 mA cm^{-2} noted by Schmidt and co-workers.[9]

In these devices, sustained photocurrent is achieved using cobalt complexes as redox mediators to reductively regenerate the ground state of the dye molecules and close the photochemical cycle. In contrast to a standard DSSC where excitation and electron injection occur at an ultrafast time scale,[14] a TTA-UC DSSC relies on long-lived triplet states that may be quenched in the presence of the redox mediator. In fact, our first TTA-UC device utilized cobalt based mediators because the conventional I^-/I_3^- mediator was found to quench TTA-UC.[7b]

Received: May 26, 2017
Published: July 31, 2017

DOI: 10.1021/jacs.7b05462
J. Am. Chem. Soc. 2017, 139, 10988−10991

Here we incorporate a series of cobalt redox shuttles into self-assembled bilayer TTA-UC DSSCs to understand their influence on the device performance, the maximum efficiency onset threshold (I_{th} value), and excited-state quenching mechanism. The redox mediators were selected because of their similar size, to mitigate any influence of their diffusion rate, and their relatively wide range of redox potentials between 0.50 and 1.20 V vs NHE (Figure 2).[15]

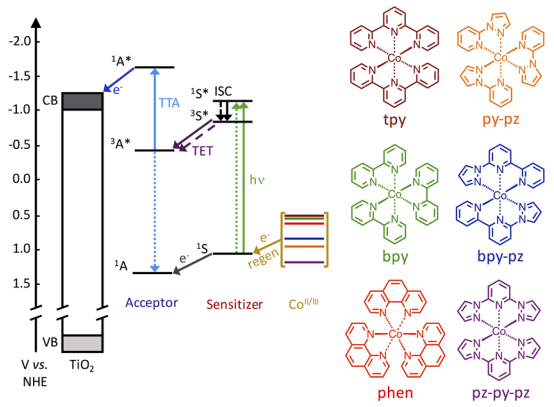

Figure 2. Electronic transitions and energetics for TiO_2, A, S, and the mediators (vs NHE) alongside the structure of the $Co^{II/III}$ redox mediators. (ISC = intersystem crossing, TET = triplet energy transfer, TTA = triplet−triplet annihilation.)

DSSCs were prepared in a standard sandwich cell architecture with TiO_2−A−Zn−S films as the photoanode (A-to-S ratio of 3:1), platinum as the counter electrode, and 0.2 M/0.02 M Co^{II}/Co^{III} redox mediator in dry, O_2-free MeCN as the electrolyte. Photocurrent density−voltage (J−V) curves (Figures S3 and S4) for DSSCs containing the various mediators were measured under AM1.5 solar irradiation passed through a 495 nm long-pass filter to isolate the contribution from TTA-UC,[7b] and the results are displayed in Table 1.

Table 1. Photovoltaic Characteristics for DSSCs Containing Cobalt Mediators under AM1.5 Solar Irradiation Passed through a 495 nm Long-Pass Filter

$Co^{II/III}$	$E_{1/2}$ (V)[a]	J_{sc} (μA cm^{-2})	V_{oc} (mV)	η (%)[b]
tpy	0.50	10.9	2.0	5.9×10^{-10}
bpy	0.54	23.6	10.0	5.2×10^{-5}
phen	0.62	158.4	110.0	6.2×10^{-3}
bpy-pz	0.83	64.7	100.0	2.0×10^{-3}
py-pz	0.96	62.0	90.0	2.0×10^{-3}
pz-py-pz	1.20	33.2	280.0	4.7×10^{-3}

[a]Oxidation potential from cyclic voltammetry (vs NHE). [b]Calculated for AM1.5 irradiation (100 mW/cm^2) and not corrected for the 495 nm filter.

In DSSCs, the V_{oc} is dictated by the energy difference between the Fermi level of the electrons within TiO_2 and the redox potential of the mediator.[16] Because all of these devices were prepared with the same TiO_2, the general trend between V_{oc} with $Co^{II/III}$ redox couple (i.e., the more positive the potential the larger the V_{oc}) is not surprising. In contrast, there is no obvious relationship between J_{sc} and the mediator potential, with tpy being the lowest (10.9 μA cm^{-2}) and phen being the highest (158.4 μA cm^{-2}). The latter result is particularly notable because it is the highest photocurrent yet achieved from TTA-UC and is above the device relevant threshold of 0.1 mA cm^{-2} under 1 sun.[9] In our previous report, the J_{sc} value was increased from 0.009 mA cm^{-2} to 0.074 mA cm^{-2} by incorporating multiple sensitizers and increasing broad band absorption.[13] The more than 2-fold increase of J_{sc} reported here, without increased absorption, clearly demonstrates the importance of the mediator in dictating TTA-UC and photocurrent generation efficiency.

For each device, the short circuit photocurrent density (J_{sc}) was measured with respect to the incident laser excitation power at 532 nm and the results can be seen in Figure 3. For all

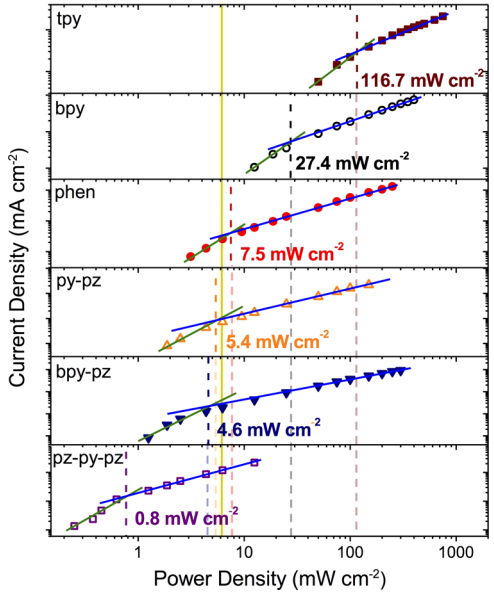

Figure 3. Short-circuit photocurrent density for TiO_2−A−Zn−S devices with respect to 532 nm excitation intensity (TiO_2 thin-film working electrode, Pt counter electrode, with $Co^{II/III}$ mediator in MeCN). Lines with slopes of 1 and 2 are shown in blue and green, respectively.

six of the mediators we observe a transition from quadratic to linear intensity dependence that is well known and a characteristic feature of TTA-UC.[17] The crossover intensity between the two regimes (vertical dashed line in Figure 3), also known as the I_{th} value, is an important metric in upconversion because it is the minimum excitation intensity threshold where TTA-UC reaches maximum efficiency for the given system.

For this series of mediators, we see a more than 2 orders of magnitude range in I_{th} values (Figure 3 and Figure S5), with the highest being 116.7 mW cm^{-2} for tpy and the lowest at 0.8 mW cm^{-2} for pz-py-pz. For solar energy conversion applications, it is desirable to achieve an I_{th} value that is below 1 sun solar intensity, which we define here as 6 mW cm^{-2} (vertical yellow line in Figure 3) from the integrated AM1.5 solar intensity over the Q-band absorption feature of S (480−535 nm). Three mediators, phen, py-pz, and bpy-pz, exhibit I_{th} values near this threshold. Particularly notable is that pz-py-pz is reaching its maximum efficiency at intensities nearly an order of magnitude lower than solar flux (0.8 mW cm^{-2}) and is on par with the lowest I_{th} value reported to date for any TTA-UC system, 0.75 mW cm^{-2}.[18]

The variables that dictate the I_{th} value in a TTA-UC system are described in eq 1:[17a]

DOI: 10.1021/jacs.7b05462
J. Am. Chem. Soc. 2017, 139, 10988−10991

$$I_{th} = \frac{1}{\alpha(E)(\tau_A^T)^2 \gamma_{TT} \Phi_{tr}} \quad (1)$$

Since all devices were prepared with similar TiO_2-A−Zn−S anodes (i.e., the same loading procedure and A and S concentrations), the absorption cross section ($\alpha(E)$) and the second-order annihilation constant (γ_{TT}) are expected to be similar regardless of the mediator. If that is the case, then the large range in I_{th} values is due to the mediator influencing either the sensitizer to acceptor energy-transfer quantum yield (Φ_{tr}) or the lifetime of the triplet state of A (τ_A^T). The correlation of I_{th} values with redox potential of the mediators (Figure S6) and the percent emission quenching (Figures S7 and S8) indicates excited-state quenching of ^{3}S* (decreasing Φ_{tr} through quenching prior to energy transfer) or A (lowering τ_A^T) may be responsible for the observed differences.

The excited-state quenching for ZrO_2−S in the presence of the $Co^{II/III}(pz\text{-}py\text{-}pz)_2$ was monitored by time-resolved emission and transient absorption spectroscopy and the results can be seen in Figure S10 and Figure 4, respectively. For these

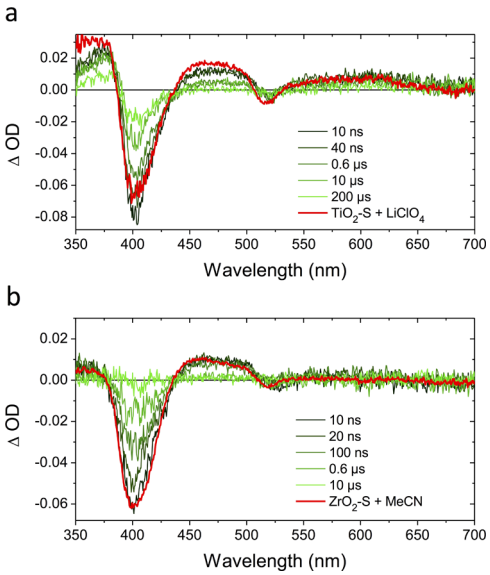

Figure 4. Full spectrum ns-TA data for sealed cells of (a) ZrO_2−S with 0.02 M $Co^{III}(pz\text{-}py\text{-}pz)_2$ in dry MeCN with overlay of TiO_2−S with 0.1 M $LiClO_4$ at 10 ns, and (b) ZrO_2−S with 0.2 M $Co^{II}(pz\text{-}py\text{-}pz)_2$ in dry MeCN with overlay of ZrO_2−S with dry MeCN at 10 ns.

measurements ZrO_2 was used as the nanocrystalline substrate to selectively monitor the excited-state quenching by the mediator in the absence of electron transfer to the metal oxide.[12]

The transient absorption spectra for ZrO_2−S in the presence of $Co^{III}(pz\text{-}py\text{-}pz)_2$ exhibits long-lived (~240 μs), positive absorption features from 350 to 380 nm and from 540 to 650 nm that are characteristic of S^+ formation (Figure 4a). Similar spectral features are seen for TiO_2−S in 0.1 M $LiClO_4$ MeCN where Li^+ is added to lower the TiO_2 conduction band and favor electron injection from S* to generate S^+.[19] These results suggest that Co^{III} mediator quenches ^{3}S* via an electron-transfer mechanism.[20] Alternatively, in the presence of $Co^{II}(pz\text{-}py\text{-}pz)_2$ only spectral features of ^{3}S* are observed, albeit they decay at a faster rate than in the absence of mediator (Figure 4b). The lack of new species suggests that quenching of ^{3}S* occurs via either energy transfer[20a,21] or paramagnetic quenching[22] to/by the Co^{II} species.

Rates of excited-state quenching of ZrO_2−S* by Co^{II} and $Co^{III}(pz\text{-}py\text{-}pz)_2$ at respective device concentrations (0.2 M:0.02 M, Co^{II}:Co^{III}) were measured using time-resolved emission (Figure S11). Despite the concentration of Co^{II} being 10 times larger, the quenching rate with Co^{II} (1.42×10^5 s^{-1}) is similar to that for Co^{III} (1.37×10^5 s^{-1}). This indicates that both oxidation states of the mediator play a role in dictating the I_{th} value. Although more difficult to measure since the triplet of A must be generated via sensitization, we anticipate similar quenching mechanisms and rates for ^{3}A*. If that is the case, the large range in I_{th} values may be due to the mediator decreasing Φ_{tr} and τ_A^T with the latter exhibiting an inverse squared contribution to I_{th}.

Interestingly there is no correlation between I_{th} value and J_{sc} for the devices. For example, despite safely operating in the linear, maximum efficiency regime, the pz-py-pz device J_{sc} is lower than that for phen, py-pz, and bpy-pz. This observation indicates that while TTA-UC may be efficient with pz-py-pz, the regeneration/recombination rate by/with the mediator may be slower/faster than the other mediators effectively reducing the light harvesting efficiency.

In conclusion, the choice of redox mediator has a large impact on the performance of TTA-UC DSSCs. The highest photocurrent enhancement yet generated from TTA-UC under 1 sun was achieved using $Co^{II/III}(phen)_3$ as the mediator. There was also >100-fold difference in I_{th} values, with the lowest, 0.8 mW cm^{-2} for $Co^{II/III}(pz\text{-}py\text{-}pz)_2(PF_6)_2$, being well below solar intensities and on par with the lowest value yet reported. The large ranges of J_{sc} and I_{th} values are attributed to triplet excited-state quenching via (1) energy transfer or paramagnetic quenching by the Co^{II} species, and (2) excited-state electron transfer to the Co^{III} species, as demonstrated by transient absorption and time-resolved emission measurements. These results demonstrate that self-assembled bilayers are a promising motif to harness low-energy light via TTA-UC. Selecting/designing redox mediators to maximize dye regeneration but inhibit recombination and excited-state quenching will be pivotal in maximizing TTA-UC DSSC efficiencies.

■ ASSOCIATED CONTENT

Supporting Information

The Supporting Information is available free of charge on the ACS Publications website at DOI: 10.1021/jacs.7b05462.

Experimental details, CV of redox mediators, device characterization data, I_{th} value relationships, full spectrum nanosecond transient absorption, and spectroelectrochemical spectra, including Figures S1−S11 (PDF)

■ AUTHOR INFORMATION

Corresponding Author

*hanson@chem.fsu.edu

ORCID

Kenneth Hanson: 0000-0001-7219-7808

Notes

The authors declare no competing financial interest.

■ ACKNOWLEDGMENTS

The authors would like to thank the Florida State University's Energy and Materials Initiative for facilitating aspects of this

DOI: 10.1021/jacs.7b05462
J. Am. Chem. Soc. 2017, 139, 10988−10991

research. Transient absorption measurements were performed on a spectrometer supported by the National Science Foundation under Grant No. CHE-1531629.

REFERENCES

(1) Shockley, W.; Queisser, H. J. *J. Appl. Phys.* **1961**, *32*, 510−519.
(2) (a) Ekins-Daukes, N. J.; Schmidt, T. W. *Appl. Phys. Lett.* **2008**, *93*, 063507. (b) Schulze, T. F.; Schmidt, T. W. *Energy Environ. Sci.* **2015**, *8*, 103−125.
(3) (a) Parker, C. A.; Hatchard, C. G. *J. Phys. Chem.* **1962**, *66*, 2506−2511. (b) Singh-Rachford, T. N.; Castellano, F. N. *Coord. Chem. Rev.* **2010**, *254*, 2560−2573.
(4) (a) Baluschev, S.; Miteva, T.; Yakutkin, V.; Nelles, G.; Yasuda, A.; Wegner, G. *Phys. Rev. Lett.* **2006**, *97*, 143903. (b) Tayebjee, M. J. Y.; McCamey, D. R.; Schmidt, T. W. *J. Phys. Chem. Lett.* **2015**, *6*, 2367−2378.
(5) Cheng, Y. Y.; Nattestad, A.; Schulze, T. F.; MacQueen, R. W.; Fuckel, B.; Lips, K.; Wallace, G. G.; Khoury, T.; Crossley, M. J.; Schmidt, T. W. *Chem. Sci.* **2016**, *7*, 559−568.
(6) (a) Cheng, Y. Y.; Fuckel, B.; MacQueen, R. W.; Khoury, T.; Clady, R. G. C. R.; Schulze, T. F.; Ekins-Daukes, N. J.; Crossley, M. J.; Stannowski, B.; Lips, K.; Schmidt, T. W. *Energy Environ. Sci.* **2012**, *5*, 6953−6959. (b) Nattestad, A.; Cheng, Y. Y.; MacQueen, R. W.; Schulze, T. F.; Thompson, F. W.; Mozer, A. J.; Fuckel, B.; Khoury, T.; Crossley, M. J.; Lips, K.; Wallace, G. G.; Schmidt, T. W. *J. Phys. Chem. Lett.* **2013**, *4*, 2073−2078. (c) Monguzzi, A.; Borisov, S. M.; Pedrini, J.; Klimant, I.; Salvalaggio, M.; Biagini, P.; Melchiorre, F.; Lelii, C.; Meinardi, F. *Adv. Funct. Mater.* **2015**, *25*, 5617−5624.
(7) (a) Simpson, C.; Clarke, T. M.; MacQueen, R. W.; Cheng, Y. Y.; Trevitt, A. J.; Mozer, A. J.; Wagner, P.; Schmidt, T. W.; Nattestad, A. *Phys. Chem. Chem. Phys.* **2015**, *17*, 24826−24830. (b) Hill, S. P.; Dilbeck, T.; Baduell, E.; Hanson, K. *ACS Energy Lett.* **2016**, *1*, 3−8.
(8) Lin, Y. L.; Koch, M.; Brigeman, A. N.; Freeman, D. M. E.; Zhao, L.; Bronstein, H.; Giebink, N. C.; Scholes, G. D.; Rand, B. P. *Energy Environ. Sci.* **2017**, *10*, 1465−1475.
(9) Frazer, L.; Gallaher, J. K.; Schmidt, T. W. *ACS Energy Lett.* **2017**, *2*, 1346−1354.
(10) (a) Lee, H.; Kepley, L. J.; Hong, H. G.; Mallouk, T. E. *J. Am. Chem. Soc.* **1988**, *110*, 618−620. (b) Terada, K.; Kobayashi, K.; Hikita, J.; Haga, M. *Chem. Lett.* **2009**, *38*, 416−417.
(11) Hanson, K.; Torelli, D. A.; Vannucci, A. K.; Brennaman, M. K.; Luo, H. L.; Alibabaei, L.; Song, W. J.; Ashford, D. L.; Norris, M. R.; Glasson, C. R. K.; Concepcion, J. J.; Meyer, T. J. *Angew. Chem., Int. Ed.* **2012**, *51*, 12782−12785.
(12) Hill, S. P.; Banerjee, T.; Dilbeck, T.; Hanson, K. *J. Phys. Chem. Lett.* **2015**, *6*, 4510−4517.
(13) Dilbeck, T.; Hill, S. P.; Hanson, K. *J. Mater. Chem. A* **2017**, *5*, 11652−11660.
(14) Asbury, J. B.; Ellingson, R. J.; Ghosh, H. N.; Ferrere, S.; Nozik, A. J.; Lian, T. Q. *J. Phys. Chem. B* **1999**, *103*, 3110−3119.
(15) (a) Sapp, S. A.; Elliott, C. M.; Contado, C.; Caramori, S.; Bignozzi, C. A. *J. Am. Chem. Soc.* **2002**, *124*, 11215−11222. (b) Mosconi, E.; Yum, J. H.; Kessler, F.; Gomez Garcia, C. J.; Zuccaccia, C.; Cinti, A.; Nazeeruddin, M. K.; Gratzel, M.; De Angelis, F. *J. Am. Chem. Soc.* **2012**, *134*, 19438−19453.
(16) Nazeeruddin, M. K.; Baranoff, E.; Gratzel, M. *Sol. Energy* **2011**, *85*, 1172−1178.
(17) (a) Monguzzi, A.; Mezyk, J.; Scotognella, F.; Tubino, R.; Meinardi, F. *Phys. Rev. B: Condens. Matter Mater. Phys.* **2008**, *78*, 195112. (b) Haefele, A.; Blumhoff, J.; Khnayzer, R. S.; Castellano, F. N. *J. Phys. Chem. Lett.* **2012**, *3*, 299−303.
(18) Duan, P. F.; Yanai, N.; Nagatomi, H.; Kimizuka, N. *J. Am. Chem. Soc.* **2015**, *137*, 1887−1894.
(19) Watson, D. F.; Meyer, G. J. *Coord. Chem. Rev.* **2004**, *248*, 1391−1406.
(20) (a) Ohno, T.; Kato, S. *J. Phys. Chem.* **1984**, *88*, 1670−1674. (b) Yoshimura, A.; Uddin, M. J.; Amasaki, N.; Ohno, T. *J. Phys. Chem. A* **2001**, *105*, 10846−10853.
(21) Krishnan, C. V.; Brunschwig, B. S.; Creutz, C.; Sutin, N. *J. Am. Chem. Soc.* **1985**, *107*, 2005−2015.
(22) (a) Porter, G.; Wright, M. R. *Discuss. Faraday Soc.* **1959**, *27*, 18. (b) Volchkov, V. V.; Ivanov, V. L.; Uzhinov, B. M. *J. Fluoresc.* **2010**, *20*, 299−303.

DOI: 10.1021/jacs.7b05462
J. Am. Chem. Soc. 2017, 139, 10988−10991